Latin American Journal of Solids and Structures
www.lajss.org

Investigation of Size-Dependency in Free-Vibration of Micro-Resonators Based on the Strain Gradient Theory

Abstract

This paper investigates the vibration behavior of micro-resonators based on the strain gradient theory, a non-classical continuum theory capable of capturing the size effect appearing in micro-scale structures. The micro-resonator is modeled as a clamped-clamped micro-beam with an attached mass subjected to an axial force. The governing equations of motion and both classical and non-classical sets of boundary conditions are developed based on the strain gradient theory. The normalized natural frequency of the micro-resonator is evaluated and the influences of various parameters are assessed. In addition, the current results are compared to those of the classical and modified couple stress continuum theories.

Keywords

Strain gradient theory; Micro-resonator; Size-dependency; Length scale parameter; Free vibration.

R. Vatankhah [a]
M.H. Kahrobaiyan [b]

[a] School of Mechanical Engineering, Shiraz University, Shiraz, Iran,
Email: rvatankhah@shirazu.ac.ir

[b] Institute of Microengineering, School of Engineering, Ecole polytechnique fédérale de Lausanne (EPFL), Lausanne, Switzerland,
Email: mohammad.kahrobaiyan@epfl.ch

http://dx.doi.org/10.1590/1679-78252430

Received 01.09.2015
Accepted 04.11.2015
Available online 09.11.2015

1 INTRODUCTION

Today, micro-scale structures such as microbeams, microplates, microbars, etc are widely used in Micro-Electro-Mechanical-Systems (MEMS) such as micro-actuators (Padoina et al., 2015), micro-switches (Joglekar, and Pawaskar, 2011), Atomic Force Microscopes (AFMs) (Kahrobaiyan et al., 2010), micro-resonators (Hassanpour et al., 2007, Ghanbari et al., 2015) and etc. Micro-resonator is a micro-scale structure supposed to vibrate at a certain frequency (usually one of its natural frequencies) and play an important role in MEMS (Hassanpour et al., 2007, Ghanbari et al., 2015). Hence, modeling the micro-resonators accurately and investigating their vibration behavior seem to be crucial.
The experimental observations have indicated that the mechanical behaviors of the micro/nano structures are size-dependent (Fleck et al., 1994, Stolken and Evans, 1998, Lam et al., 2003). Since the classical continuum mechanics is incapable of capturing the size effect and consequently unable to predict and interpret the size-dependent static and vibration behavior observed in micro-scale structures, during

past years, some non-classical continuum theories such as the nonlocal, strain gradient and couple stress theories have been introduced, developed and employed to study the micro-scale structures. In these non-classical theories, some material parameters are considered in addition to the two classical parameters, elastic modulus and Poisson ratio, which enable these theories to capture the size-dependency. For example, in the modified couple stress theory, due to the micro structure rotation gradient, an additional length scale parameter is considered while in the strain gradient theory, there exist three additional length scale parameters corresponding to the micro structure rotation gradient, the micro structure dilatation gradient and the micro structure stretch gradient.

Since the characteristic length of micro-resonators is in the order of microns or sub-microns, their mechanical behavior is size-dependent. So, investigating the size-dependency in micro-resonators by applying some non-classical continuum theory, such as the strain gradient theory, seems to be necessary. In this paper, the strain gradient theory is employed as a non-classical theory to study the size-dependent vibration behavior of micro-resonators. Hereafter, a literature review on the non-classical continuum theories is presented:

The couple stress theory is a non-classical continuum theory in which higher-order stresses, known as the couple stresses exist (Asghari et al., 2011). A modified couple stress theory has been proposed by Yang et al. (2002) in which a new higher-order equilibrium equation, i.e. the equilibrium equation of moments of couples, is considered in addition to the classical equilibrium equations of forces and moments of forces. This theory has been employed to formulate the size-dependent static and dynamic behavior of linear and nonlinear Euler-Bernoulli and Timoshenko microbeams (Park and Gao, 2006, Ma et al., 2008, Asghari et al., 2010, Liang et al., 2015), linear homogenous Kirchhoff microplates (Tsiatas, 2009, Ansari et al., 2014), buckling of composite laminated beams (Abadi and Daneshmehr, 2014), and also nonlinear three dimensional curved microtubes (Tang et al., 2014). Recently, static pull-in instability and free vibration of electrostatically actuated microplates are studied based on the modified couple stress theory (Wang et al., 2015).

In a similar way utilized by Yang et al. (2002) for the modification of the couple stress theory, Lam et al. (2003) introduced a modified strain gradient theory, which reduces in a special case to the modified couple stress theory. Henceforth, when the strain gradient theory is used in the text, it denotes the version of the theory presented by Lam et al. (2003).

In the strain gradient theory, there exist three length scale parameters corresponding to the micro structure rotation gradient, the micro structure dilatation gradient and the micro structure stretch gradient. In studies associated with the strain gradient theory, for numerical evaluations, the researchers usually consider these three length scale parameters to be the same and indeed equal to the length scale parameter used in the modified couple stress theory (Kong et al., 2009, Koochi et al., 2014). In order to determine the length scale parameter for a specific material, some typical experiments such as micro-bend test, micro-torsion test and specially micro/nano indentation test can be carried out. As an example, according to the micro-torsion test of thin copper wire (Fleck et al., 1994), the copper length scale parameter has been reported $4\mu m$. Also, according to the micro-bend test of thin nickel and epoxy beams, the length scale parameter for nickel and epoxy has been estimated $5\mu m$ (Stolken and Evans, 1998) and 17.6 μm (Lam et al., 2003), respectively. Utilizing the micro-indentation experiments performed by McElhaney et al. (1998), Nix and Gao (1998) evaluated the material length

scale parameter of annealed single crystal copper and cold worked polycrystalline copper to be 12 μm and 5.84 μm, respectively.

The strain gradient theory is utilized to formulate the static and dynamic behaviors of linear Euler-Bernoulli by Kong et al. (2009). The torsional static and dynamic behavior of microbars is investigated by Kahrobaiyan et al. (2011) using the strain gradient theory. Vatankhah et al. (2013a, 2014a, 2014b, 2015a, 2015b) presented the problem of vibration control strain gradient micro-scale beams. In addition, employing the strain gradient theory, the size-dependent nonlinear forced vibration of a vibrating non-classical Euler–Bernoulli micro-beam has been investigated by Vatankhah et al. (2013b).

In this paper, based on the strain gradient theory, the size-dependent free vibration of micro-resonators is studied. The results are compared to those of the modified couple stress and classical theories and the effects of different parameters such as the length scale parameter and the design parameters like the gyration radius of the attached mass are assessed on the frequency of micro-resonators.

2 PRELIMINARIES

According to the strain gradient theory proposed by Lam et al. (2003), the stored strain energy U for a linear elastic material occupying region Ω having infinitesimal deformations is written as (Vatankhah et al., 2013b):

$$U = \int_{\Omega} \overline{u}\, dv = \frac{1}{2}\int_{\Omega} \left(\sigma_{ij}\varepsilon_{ij} + p_i\gamma_i + \tau^{(1)}_{ijk}\ \eta^{(1)}_{ijk} + m^{s}_{ij}\ \chi^{s}_{ij} \right) dv \tag{1}$$

where

$$\varepsilon_{ij} = \frac{1}{2}\left(u_{i,j} + u_{j,i} \right) \tag{2}$$

$$\gamma_i = \varepsilon_{mm,i} \tag{3}$$

$$\begin{aligned} \eta^{(1)}_{ijk} = {} & \frac{1}{3}\left(\varepsilon_{jk,i} + \varepsilon_{ki,j} + \varepsilon_{ij,k} \right) - \frac{1}{15}\delta_{ij}\left(\varepsilon_{mm,k} + 2\varepsilon_{mk,m} \right) \\ & - \frac{1}{15}\left[\delta_{jk}\left(\varepsilon_{mm,i} + 2\varepsilon_{mi,m} \right) + \delta_{ki}\left(\varepsilon_{mm,j} + 2\varepsilon_{mj,m} \right) \right] \end{aligned} \tag{4}$$

$$\chi^{s}_{ij} = \frac{1}{2}\left(\varphi_{i,j} + \varphi_{j,i} \right) \tag{5}$$

$$\varphi_i = \frac{1}{2}\left(curl\left(\mathrm{u} \right) \right)_i \tag{6}$$

where u_i, γ_i and θ_i denote the components of the displacement vector u, the dilatation gradient vector $\boldsymbol{\gamma}$, and the infinitesimal rotation vector $\boldsymbol{\varphi}$. Also, the components of the strain tensor $\boldsymbol{\varepsilon}$, the deviatoric stretch gradient tensor $\boldsymbol{\eta}^{(1)}$, and the symmetric part of the rotation gradient tensor $\boldsymbol{\chi}^{s}$ are

represented by ε_{ij}, $\eta^{(1)}_{ijk}$ and χ^{s}_{ij}. The parameters which are obtained by differentiating the strain energy density with respect to kinematics parameters $\boldsymbol{\varepsilon}$, $\boldsymbol{\gamma}$, $\boldsymbol{\eta}^{(1)}$ and $\boldsymbol{\chi}^{s}$ are, respectively, symbolized by $\boldsymbol{\sigma}$, p, $\boldsymbol{\tau}^{(1)}$ and m^{s}. The parameters p, $\boldsymbol{\tau}^{(1)}$ and m^{s} are usually called the higher-order stresses. According to the constitutive equations for a linear isotropic elastic material, the components of the stresses are related to the kinematic parameters effective on $\overline{u}$ as follows (Lam et al., 2003)

$$\sigma_{ij} = \lambda tr\left(\boldsymbol{\varepsilon}\right)\delta_{ij} + 2\mu\varepsilon_{ij} \tag{7}$$

$$p_i = 2\mu l_0^{\,2}\gamma_i \tag{8}$$

$$\tau^{(1)}_{ijk} = 2\mu l_1^{\,2}\eta^{(1)}_{ijk} \tag{9}$$

$$m^{s}_{ij} = 2\mu l_2^{\,2}\chi^{s}_{ij} \tag{10}$$

In above equations, the Lame constants appeared in the constitutive equation of the classical stress $\boldsymbol{\sigma}$ are denoted by λ and μ. Also, the additional independent material length scale parameters appeared in the constitutive equations of higher order stresses are represented by l_0, l_1, and l_2. The Lame constants can be written in terms of the Young modulus E and the Poisson ratio υ as $\lambda = \nu E / (1+\upsilon)(1-2\upsilon)$ and $\mu = E / 2(1+\upsilon)$.

For a linear Euler-Bernoulli beam with uniform cross-section A and length L subjected to a uniform axial load P and distributed lateral load $F\left(x,t\right)$, the governing equation of motion and boundary conditions are derived as (Vatankhah et al., 2013b):

$$S\frac{\partial^4 w}{\partial x^4} - K\frac{\partial^6 w}{\partial x^6} - P\frac{\partial^2 w}{\partial x^2} + \rho A\frac{\partial^2 w}{\partial t^2} = F\left(x,t\right) \tag{11}$$

$$\left(P\frac{\partial w}{\partial x} - S\frac{\partial^3 w}{\partial x^3} + K\frac{\partial^5 w}{\partial x^5} - \hat{V}\right)\Bigg|_{x=0,L} = 0, \quad \text{or} \quad \delta w\big|_{x=0,L} = 0\,, \tag{12}$$

$$\left(S\frac{\partial^2 w}{\partial x^2} - K\frac{\partial^4 w}{\partial x^4} - \hat{M}\right)\Bigg|_{x=0,L} = 0 \qquad \text{or} \qquad \delta\left(\frac{\partial w}{\partial x}\right)\Bigg|_{x=0,L} = 0\,, \tag{13}$$

$$\left(K\frac{\partial^3 w}{\partial x^3} - \hat{Q}^{h}\right)\Bigg|_{x=0,L} = 0 \qquad \text{or} \qquad \delta\left(\frac{\partial^2 w}{\partial x^2}\right)\Bigg|_{x=0,L} = 0\,. \tag{14}$$

where ρ denotes the beam density, w represents the lateral deflection, $\hat{V}$ stand for the resultant transverse forces in a section caused by the classical stress components acting on the section, $\hat{Q}^{h}$ refers to the higher-order resultants in a section, work conjugate to $\partial^2 w / \partial x^2$, caused by higher-order stresses acting on the section and $\hat{M}$ is the resultant moment in a section caused by the classical and higher-order stress components. Also:

$$S = EI + \mu A\left(2{l_0}^2 + \frac{8}{15}{l_1}^2 + {l_2}^2\right), \tag{15}$$

$$K = \mu I\left(2{l_0}^2 + \frac{4}{5}{l_1}^2\right), \tag{16}$$

in which I denotes the area moment of inertia of the beam cross-section defined as: $I = \int_A z^2 dA$.

3 MODELING

In this section, the free-vibration characteristics of a micro-resonator are going to be investigated. To that end, consider a micro-resonator modeled as a clamped-clamped Euler-Bernoulli beam having a concentrated mass attached along its length and subjected to a tensile axial load (see figure 1).

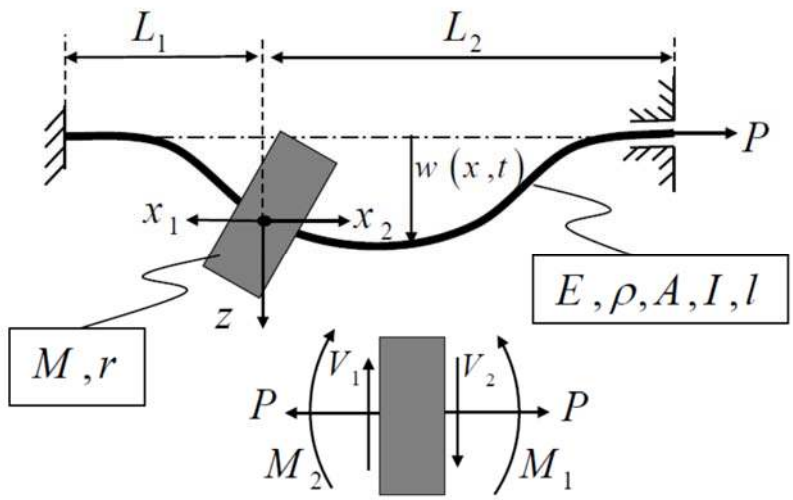


Figure 1: A micro-resonator: Geometry, coordinate system, kinematic parameters and resultants acting on the attached mass.

In this figure, P refers to the tensile axial load. In addition, M and r respectively denote the value and gyration radius of the attached mass. Moreover, the beam length is represented by L where L_1 stands for the length of the beam from the attached mass up to the left clamped end and L_2 denotes the length of the beam from the attached mass up to the right clamped end as indicated in the figure. Normalization of the governing equation of motion mentioned in Eq. (11) would be helpful. Hence, utilizing the following dimensionless parameters:

$$\tilde{P} = \frac{PL^2}{2EI}, \quad \tilde{x} = \frac{x}{L}, \quad \tilde{t} = \frac{t}{L^2}\sqrt{\frac{EI}{\rho A}}, \quad \tilde{w}(\tilde{x},\tilde{t}) = \frac{w(x,t)}{L} \tag{17}$$

equation (11) changes into the following normalized form:

$$\tilde{S}\frac{\partial^4 \tilde{w}}{\partial \tilde{x}^4} - \tilde{K}\frac{\partial^6 \tilde{w}}{\partial \tilde{x}^6} - 2\tilde{P}\frac{\partial^2 \tilde{w}}{\partial \tilde{x}^2} + \frac{\partial^2 \tilde{w}}{\partial \tilde{t}^2} = 0\,, \quad 0 \le \tilde{x} \le 1\,, \quad \tilde{t} \ge 0\,, \tag{18}$$

where

$$\tilde{S} = 1 + \frac{\mu A}{EI}\left(2{l_0}^2 + \frac{8}{15}{l_1}^2 + {l_2}^2\right), \tag{19}$$

$$\tilde{K} = \frac{\mu}{EL^2}\left(2{l_0}^2 + \frac{4}{5}{l_1}^2\right), \tag{20}$$

noted that in previous equations, the dimensionless axial load, longitude coordinate, time and lateral deflection are represented by $\tilde{P}$, $\tilde{x}$, $\tilde{t}$ and $\tilde{w}$ respectively.

In order to deal with the problem, the beam is considered to be made of two separated beams as depicted in figure 1. The normalized form of the governing equation of motion of the left beam can be expressed as:

$$\tilde{S}\frac{\partial^4 \tilde{w}_1}{\partial \tilde{x}_1^4} - \tilde{K}_1\frac{\partial^6 \tilde{w}_1}{\partial \tilde{x}_1^6} - 2\tilde{P}_1\frac{\partial^2 \tilde{w}_1}{\partial \tilde{x}_1^2} + \frac{\partial^2 \tilde{w}_1}{\partial \tilde{t}_1^2} = 0\,, \quad 0 \le \tilde{x}_1 \le 1\,, \quad \tilde{t}_1 \ge 0\,, \tag{21}$$

where

$$\tilde{K}_1 = \frac{\mu}{E{L_1}^2}\left(2{l_0}^2 + \frac{4}{5}{l_1}^2\right), \tag{22}$$

and

$$\tilde{P}_1 = \frac{PL_1^2}{2EI}\,, \qquad \tilde{x}_1 = \frac{x_1}{L_1}\,, \qquad \tilde{t}_1 = \frac{t_1}{L_1^2}\sqrt{\frac{EI}{\rho A}}\,, \qquad \tilde{w}_1(\tilde{x}_1,\tilde{t}_1) = \frac{w_1(x_1,t)}{L_1} \tag{23}$$

in which L_1 denotes the length of the left beam and x_1 is shown in figure 1.

Using separation of variables approach, one can express:

$$\tilde{w}_1(\tilde{x}_1,\tilde{t}_1) = \tilde{Y}_1(\tilde{x}_1)\tilde{T}_1(\tilde{t}_1)\,, \qquad \tilde{Y}_1(\tilde{x}_1) = \frac{Y_1(x_1)}{L_1}\,, \tag{24}$$

where Y_1 and $\tilde{T}_1$ are the parts of the deflection associated with the longitude coordinate and time respectively. Substituting Eq. (24) into Eq. (21) leads to:

$$\frac{d^2\tilde{T}_1}{d\tilde{t}_1^2} + \tilde{\omega}_1^2\tilde{T}_1 = 0\,, \tag{25}$$

$$\tilde{S}\frac{d^4\tilde{Y}_1}{d\tilde{t}_1^4} - \tilde{K}_1\frac{d^6\tilde{Y}_1}{d\tilde{t}_1^6} - 2\tilde{P}_1\frac{d^2\tilde{Y}_1}{d\tilde{t}_1^2} - \tilde{\omega}_1^2\tilde{Y}_1 = 0\,, \tag{26}$$

where

$$\tilde{\omega}_1 = \omega L_1^2 \sqrt{\frac{\rho A}{EI}}\,. \tag{27}$$

The solutions of Eqs. (25) and (26) are respectively:

$$\tilde{T}_1(\tilde{t}_1) = a_1 \cos\tilde{\omega}_1\tilde{t}_1 + b_1 \sin\tilde{\omega}_1\tilde{t}_1\,, \tag{28}$$

$$\tilde{Y}_1(\tilde{x}_1) = c_1 e^{\lambda_1\tilde{x}_1} + c_2 e^{\lambda_2\tilde{x}_1} + c_3 e^{\lambda_3\tilde{x}_1} + c_4 e^{\lambda_4\tilde{x}_1} + c_5 e^{\lambda_5\tilde{x}_1} + c_6 e^{\lambda_6\tilde{x}_1}\,, \tag{29}$$

where a_1, b_1 and c_i $i = 1,...6$ are some constants that can be determined by applying appropriate initial and boundary conditions. In addition, λ_i $i = 1,...,6$ can be determined from the following characteristic equation:

$$-\tilde{K}_1\tilde{\lambda}_1^6 + \tilde{S}\tilde{\lambda}_1^4 - 2\tilde{P}_1\tilde{\lambda}_1^2 - \tilde{\omega}_1^2 = 0\,. \tag{30}$$

The same procedure as the one carried out for the left beam can be done for the right beam. The normalized governing equation of motion of the right beam is expressed as:

$$\tilde{S}\frac{\partial^4\tilde{w}_2}{\partial\tilde{x}_2^4} - \tilde{K}_2\frac{\partial^6\tilde{w}_2}{\partial\tilde{x}_2^6} - 2\tilde{P}_2\frac{\partial^2\tilde{w}_2}{\partial\tilde{x}_2^2} + \frac{\partial^2\tilde{w}_2}{\partial\tilde{t}_2^2} = 0\,, \quad 0 \le \tilde{x}_2 \le 1\,, \quad \tilde{t}_2 \ge 0 \tag{31}$$

where

$$\tilde{K}_2 = \frac{\mu}{EL_2^2}\left(2{l_0}^2 + \frac{4}{5}{l_1}^2\right), \tag{32}$$

$$\tilde{P}_2 = \frac{PL_2^2}{2EI}, \qquad \tilde{x}_2 = \frac{x_2}{L_2}, \qquad \tilde{t}_2 = \frac{t_2}{L_2^2}\sqrt{\frac{EI}{\rho A}}, \qquad \tilde{w}_2(\tilde{x}_2,\tilde{t}_2) = \frac{w_2(x_2,t)}{L_2}, \tag{33}$$

in which L_2 denotes the length of the right beam and x_2 represents the longitude coordinate of the right beam depicted in figure 1. Applying the separation of variables approach to Eq. (31) as:

$$\tilde{w}_2(\tilde{x}_2,\tilde{t}_2) = \tilde{Y}_2(\tilde{x}_2)\tilde{T}_2(\tilde{t}_2)\,, \qquad \tilde{Y}_2(\tilde{x}_2) = \frac{Y_2(x_2)}{L_2}, \tag{34}$$

results in

$$\frac{d^2\tilde{T}_2}{d\tilde{t}_2^2} + \tilde{\omega}_2^2\tilde{T}_2 = 0\,, \tag{35}$$

$$\tilde{S}\frac{d^4\tilde{Y}_2}{d\tilde{t}_2^4} - \tilde{K}_2\frac{d^6\tilde{Y}_2}{d\tilde{t}_2^6} - 2\tilde{P}_2\frac{d^2\tilde{Y}_2}{d\tilde{t}_2^2} - \tilde{\omega}_2^2\tilde{Y}_2 = 0\,, \tag{36}$$

where

$$\tilde{\omega}_2 = \omega L_2^2\sqrt{\frac{\rho A}{EI}}\,. \tag{37}$$

Equation (35) and (36) are linear homogenous differential equations with constant coefficients that respectively have solutions as:

$$\tilde{T}_2(\tilde{t}_2) = a_2 \cos\tilde{\omega}_2\tilde{t}_2 + b_2 \sin\tilde{\omega}_2\tilde{t}_2\,, \tag{38}$$

$$\tilde{Y}_2(\tilde{x}_2) = c_7 e^{\lambda_7\tilde{x}_2} + c_8 e^{\lambda_8\tilde{x}_2} + c_9 e^{\lambda_9\tilde{x}_2} + c_{10} e^{\lambda_{10}\tilde{x}_2} + c_{11} e^{\lambda_{11}\tilde{x}_2} + c_{12} e^{\lambda_{12}\tilde{x}_2}\,. \tag{39}$$

It is noted that in Eqs. (38) and (39), where a_2, b_2 and c_i $i = 7,...,12$ are some constants that can be determined by applying appropriate initial and boundary conditions whereas λ_i $i = 7,...,12$, can be obtained from the characteristic equation of Eq. (36) that would be

$$-\tilde{K}_2\tilde{\lambda}_2^6 + \tilde{S}\tilde{\lambda}_2^4 - 2\tilde{P}_2\tilde{\lambda}_2^2 - \tilde{\omega}_2^2 = 0\,. \tag{40}$$

Now, the boundary conditions of the micro-beam are applied in order to determine its natural frequencies and mode shapes. The normalized boundary conditions of the left-side clamped end of beam is

$$\tilde{Y}_1\Big|_{\tilde{x}_1=1} = 0, \qquad \frac{d\tilde{Y}_1}{d\tilde{x}_1}\Big|_{\tilde{x}_1=1} = 0, \qquad \frac{d^3\tilde{Y}_1}{d\tilde{x}_1^3}\Big|_{\tilde{x}_1=1} = 0\,, \tag{41}$$

in which the first and the second terms are respectively associated with the zero deflection and zero slope of the clamped end while the third term is the non-classical boundary conditions appearing due to the implementation of the strain gradient theory of elasticity.

Similarly, the boundary conditions of the right-side clamped end would be

$$\tilde{Y}_2\Big|_{\tilde{x}_2=1} = 0, \qquad \frac{d\tilde{Y}_2}{d\tilde{x}_2}\Big|_{\tilde{x}_2=1} = 0, \qquad \frac{d^3\tilde{Y}_2}{d\tilde{x}_2^3}\Big|_{\tilde{x}_2=1} = 0\,. \tag{42}$$

Since the micro-beam composed of the left and the right beams is continuous, the continuity conditions should be applied to the left and right beams. Henceforward, the boundary conditions ensuring the micro-beam to be continuous at the origin of the left and right beams will be presented. The continuity conditions of the deflection of the micro-beam at the origin are expressed as:

$$Y_1\Big|_{x_1=0} = Y_2\Big|_{x_2=0} \Rightarrow \tilde{Y}_1\Big|_{\tilde{x}_1=0} - \frac{1}{\ell}\tilde{Y}_2\Big|_{\tilde{x}_2=0} = 0\,, \qquad \ell = \frac{L_1}{L_2}\,. \tag{43}$$

Moreover, one can express the continuity conditions of the beam slope at the origin as

$$\frac{dY_1}{dx_1}\Big|_{x_1=0} = -\frac{dY_2}{dx_2}\Big|_{x_2=0} \Rightarrow \frac{d\tilde{Y}_1}{d\tilde{x}_1}\Big|_{\tilde{x}_1=0} + \frac{d\tilde{Y}_2}{d\tilde{x}_2}\Big|_{\tilde{x}_2=0} = 0\,. \tag{44}$$

In addition, considering figure 1, the equilibrium equations along z-axis and about y-axis are respectively as follows:

$$\begin{aligned}&-V_1\Big|_{x_1=0}-V_2\Big|_{x_2=0}=M\omega^2Y_1\Big|_{x_1=0}\Rightarrow\\&\left(S\frac{d^3Y_1}{dx_1^3}-K_1\frac{d^5Y_1}{dx_1^5}\right)\Big|_{x_1=0}+\left(S\frac{d^3Y_2}{dx_2^3}-K_2\frac{d^5Y_2}{dx_2^5}\right)\Big|_{x_2=0}=M\omega^2Y_1\Big|_{x_1=0}\end{aligned},\tag{45}$$

$$\begin{aligned}&M_1\Big|_{x_1=0}-M_2\Big|_{x_2=0}=MR^2\omega^2\frac{dY_1}{dx_1}\Big|_{x_1=0}\Rightarrow\\&\left(S\frac{d^2Y_1}{dx_1^2}-K_1\frac{d^4Y_1}{dx_1^4}\right)\Big|_{x_1=0}-\left(S\frac{d^2Y_2}{dx_2^2}-K_2\frac{d^4Y_2}{dx_2^4}\right)\Big|_{x_2=0}=MR^2\omega^2\frac{dY_1}{dx_1}\Big|_{x_1=0}\end{aligned},\tag{46}$$

in which V_i and M_i $i=1,2$ respectively denote the shear force and bending moment acting on the beam sections.

Equations (45) and (46) can be rewritten in the following forms:

$$\begin{aligned}&-V_1\Big|_{x_1=0}-V_2\Big|_{x_2=0}=M\omega^2Y_1\Big|_{x_1=0}\Rightarrow\\&\left(S\frac{d^3Y_1}{dx_1^3}-K_1\frac{d^5Y_1}{dx_1^5}\right)\Big|_{x_1=0}+\left(S\frac{d^3Y_2}{dx_2^3}-K_2\frac{d^5Y_2}{dx_2^5}\right)\Big|_{x_2=0}=M\omega^2Y_1\Big|_{x_1=0}\end{aligned},\tag{47}$$

$$\left(\tilde{S}\frac{d^3\tilde{Y}_1}{d\tilde{x}_1^3}-\tilde{K}_1\frac{d^5\tilde{Y}_1}{d\tilde{x}_1^5}\right)\Big|_{\tilde{x}_1=0}+\left(\tilde{S}\frac{d^3\tilde{Y}_2}{d\tilde{x}_2^3}-\tilde{K}_2\frac{d^5\tilde{Y}_2}{d\tilde{x}_2^5}\right)\Big|_{\tilde{x}_2=0}=\alpha\omega_1^2\tilde{Y}_1\Big|_{\tilde{x}_1=0},\tag{48}$$

where

$$\alpha=\frac{M}{\rho AL_1},\qquad \beta=\frac{r}{L_1}.\tag{49}$$

The equality of the higher-order (non-classical) moments at the left and right sides of the origin, M_1^h, M_2^h, results in:

$$M_1^h(x_1)=M_2^h(x_2)=0\Rightarrow\frac{d^3Y_1}{dx_1^3}\Big|_{x_1=0}=\frac{d^3Y_2}{dx_2^3}\Big|_{x_2=0}\Rightarrow\frac{d^3\tilde{Y}_1}{d\tilde{x}_1^3}\Big|_{\tilde{x}_1=0}-\ell^2\frac{d^3\tilde{Y}_2}{d\tilde{x}_2^3}\Big|_{\tilde{x}_2=0}=0.\tag{50}$$

Furthermore, the continuity of the non-classical kinematic parameter of the micro-beam at the left and right sides of the origin, d^2Y_1/dx_1^2 and d^2Y_2/dx_2^2 leads to:

$$\frac{d^2Y_1}{dx_1^2}\Big|_{x_1=0}=\frac{d^2Y_2}{dx_2^2}\Big|_{x_2=0}\Rightarrow\frac{d^2\tilde{Y}_1}{d\tilde{x}_1^2}\Big|_{\tilde{x}_1=0}-\ell\frac{d^2\tilde{Y}_2}{d\tilde{x}_2^2}\Big|_{\tilde{x}_2=0}=0.\tag{51}$$

It is noted that Eqs. (50) and (51) appear due to employing the strain gradient theory of elasticity to investigate the vibration behavior of the micro-resonators.

Applying the boundary conditions introduced in Eqs. (41)-(51) to the Eqs. (29) and (39), the following homogenous set of algebraic equations is achieved:

$$\left[A\right]_{12\times12}\left[c_1,\, c_2,\, c_3,\, c_4,\, c_5,\, c_6,\, c_7,\, c_8,\, c_9,\, c_{10},\, c_{11},\, c_{12}\right]^{T}_{12\times1} = \left[0\right]_{12\times1}, \tag{52}$$

in which the components of the matrix $[A]$, a_{ij} $i,j = 1,...,12$ are:

$$\begin{aligned}
&a_{1,1} = e^{\lambda_1},\ a_{1,2} = e^{\lambda_2},\ a_{1,3} = e^{\lambda_3},\ a_{1,4} = e^{\lambda_4},\ a_{1,5} = e^{\lambda_5},\ a_{1,6} = e^{\lambda_6},\\
&a_{1,7} = 0,\ a_{1,8} = 0,\ a_{1,9} = 0,\ a_{1,10} = 0,\ a_{1,11} = 0,\ a_{1,12} = 0,\\
&a_{2,1} = \lambda_1 e^{\lambda_1},\ a_{2,2} = \lambda_2 e^{\lambda_2},\ a_{2,3} = \lambda_3 e^{\lambda_3},\ a_{2,4} = \lambda_4 e^{\lambda_4},\ a_{2,5} = \lambda_5 e^{\lambda_5},\ a_{2,6} = \lambda_6 e^{\lambda_6},\\
&a_{2,7} = 0,\ a_{2,8} = 0,\ a_{2,9} = 0,\ a_{2,10} = 0,\ a_{2,11} = 0,\ a_{2,12} = 0,\\
&a_{3,1} = \lambda_1^3 e^{\lambda_1},\ a_{3,2} = \lambda_2^3 e^{\lambda_2},\ a_{3,3} = \lambda_3^3 e^{\lambda_3},\ a_{3,4} = \lambda_4^3 e^{\lambda_4},\ a_{3,5} = \lambda_5^3 e^{\lambda_5},\ a_{3,6} = \lambda_6^3 e^{\lambda_6},\\
&a_{3,7} = 0,\ a_{3,8} = 0,\ a_{3,9} = 0,\ a_{3,10} = 0,\ a_{3,11} = 0,\ a_{3,12} = 0,\\
&a_{4,1} = 0,\ a_{4,2} = 0,\ a_{4,3} = 0,\ a_{4,4} = 0,\ a_{4,5} = 0,\ a_{4,6} = 0,\\
&a_{4,7} = e^{\lambda_7},\ a_{4,8} = e^{\lambda_8},\ a_{4,9} = e^{\lambda_9},\ a_{4,10} = e^{\lambda_{10}},\ a_{4,11} = e^{\lambda_{11}},\ a_{4,12} = e^{\lambda_{12}},\\
&a_{5,1} = 0,\ a_{5,2} = 0,\ a_{5,3} = 0,\ a_{5,4} = 0,\ a_{5,5} = 0,\ a_{5,6} = 0,\\
&a_{5,7} = \lambda_7 e^{\lambda_7},\ a_{5,8} = \lambda_8 e^{\lambda_8},\ a_{5,9} = \lambda_9 e^{\lambda_9},\ a_{5,10} = \lambda_{10} e^{\lambda_{10}},\ a_{5,11} = \lambda_{11} e^{\lambda_{11}},\ a_{5,12} = \lambda_{12} e^{\lambda_{12}},\\
&a_{6,1} = 0,\ a_{6,2} = 0,\ a_{6,3} = 0,\ a_{6,4} = 0,\ a_{6,5} = 0,\ a_{6,6} = 0,\\
&a_{6,7} = \lambda_7^3 e^{\lambda_7},\ a_{6,8} = \lambda_8^3 e^{\lambda_8},\ a_{6,9} = \lambda_9^3 e^{\lambda_9},\ a_{6,10} = \lambda_{10}^3 e^{\lambda_{10}},\ a_{6,11} = \lambda_{11}^3 e^{\lambda_{11}},\ a_{6,12} = \lambda_{12}^3 e^{\lambda_{12}},\\
&a_{7,1} = 1,\ a_{7,2} = 1,\ a_{7,3} = 1,\ a_{7,4} = 1,\ a_{7,5} = 1,\ a_{7,6} = 1,
\end{aligned} \tag{53}$$

Noted that eigen-values and eigen-vectors of the matrix $[A]$ respectively give the natural frequencies and mode shapes of the micro-resonator.

4 RESULTS AND DISCUSSION

In this section, the natural frequency of the micro-resonator is going to be evaluated and the effects of different parameters such as, the normalized axial load p, the normalized mass m, the normalized position of the attached mass γ and the normalized gyration radius η on the normalized natural frequency of the micro-resonator $\tilde{\omega}$ are assessed. The aforementioned dimensionless parameters are defined as:

$$m = \frac{M}{\rho A(L_1 + L_2)},\ \eta = \frac{r}{(L_1 + L_2)},\ p = \frac{P(L_1 + L_2)^2}{2EI},\ \gamma = \frac{L_1}{L_1 + L_2},\ \tilde{\omega} = \omega(L_1 + L_2)\sqrt{\frac{\rho A}{EI}}. \tag{54}$$

The normalized natural frequency of the micro-resonator is respectively delineated as a function of the normalized axial load, mass, attached mass position and gyration radius in Figures 2-5 for various values of the ratio of the beam thickness to the material length scale parameter h / l. It is considered that the ratio of the beam width b to the beam thickness h to be $b / h = 5$.

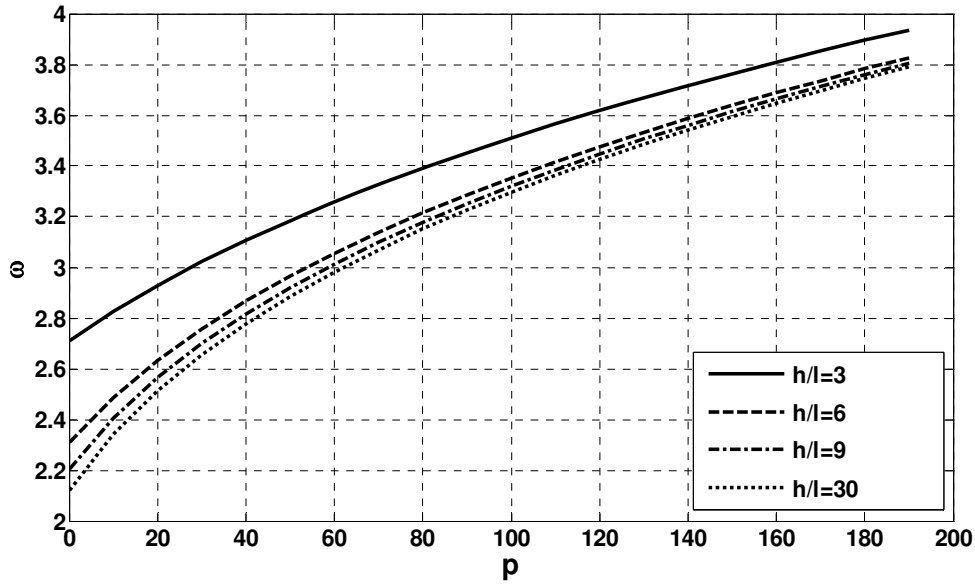


Figure 2: The micro-resonator normalized natural frequency versus the normalized axial load for various values of the ratio of the microbeam thickness to the length scale parameter.

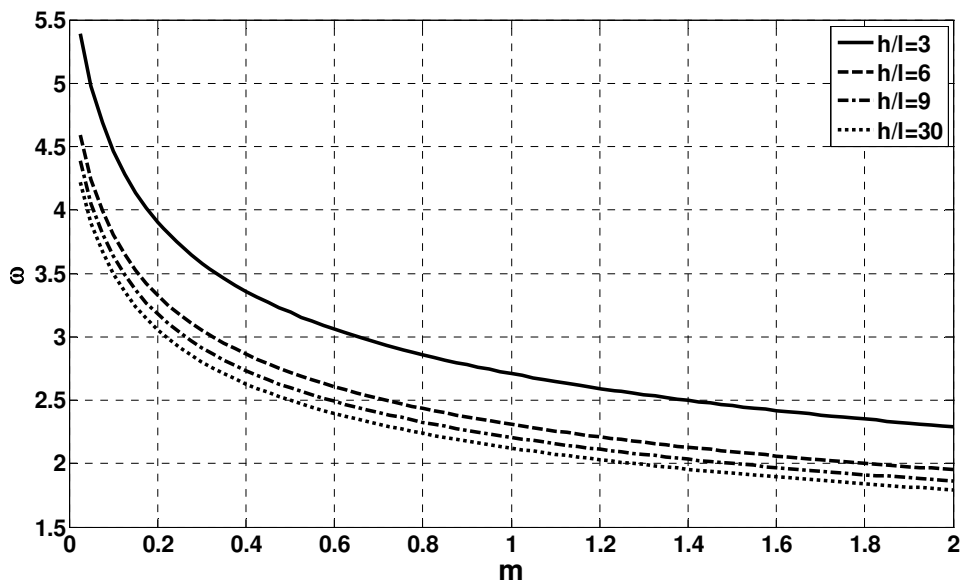


Figure 3: The micro-resonator normalized natural frequency versus the normalized mass for various values of the ratio of the microbeam thickness to the length scale parameter.

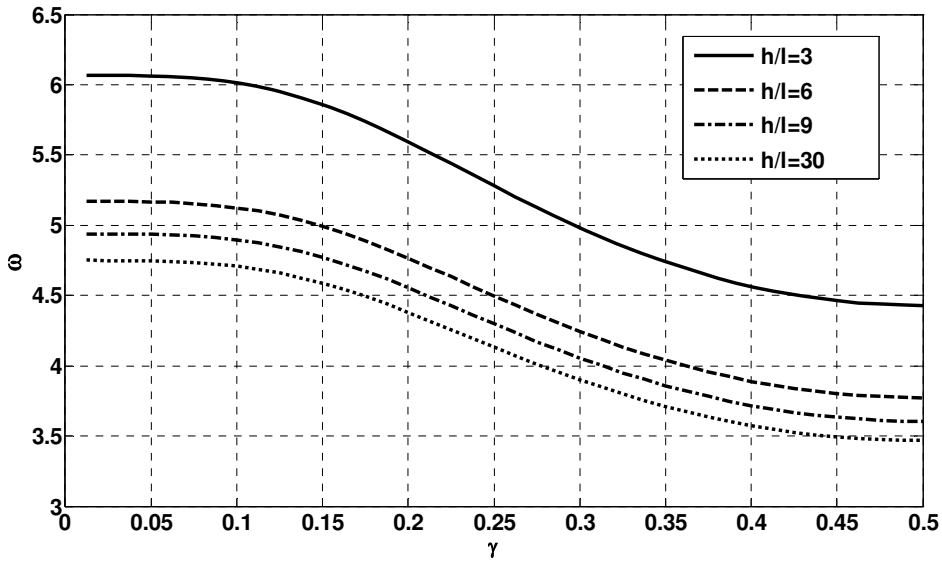


Figure 4: The micro-resonator normalized natural frequency versus the normalized position of the attached mass for various values of the ratio of the microbeam thickness to the length scale parameter.

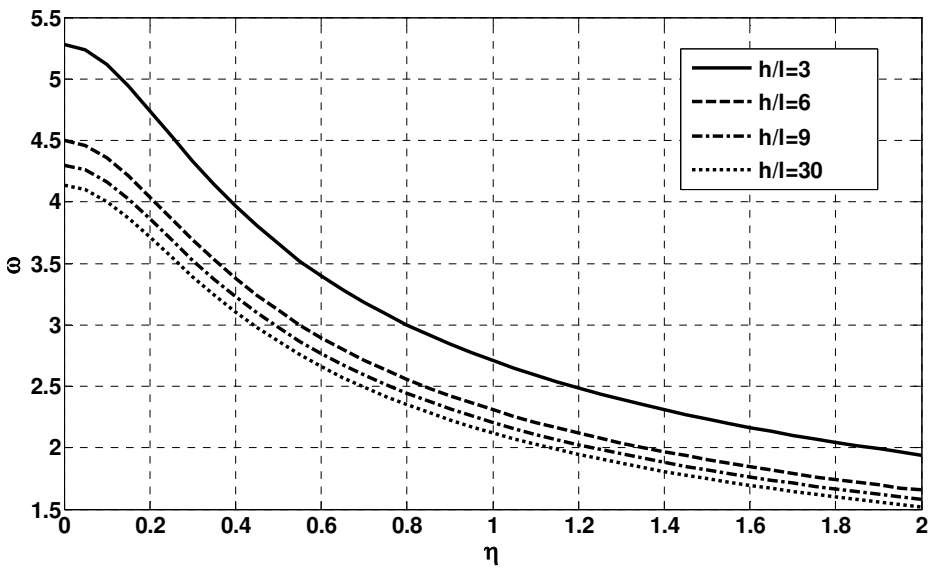


Figure 5: The micro-resonator normalized natural frequency versus the normalized gyration radius of the attached mass for various values of the ratio of the microbeam thickness to the length scale parameter.

Figures 2-5 indicate that the vibration behavior of the micro-beam of the micro-resonator is size-dependent and as the ratio of the beam thickness to the material length scale decreases, the frequency increases. Form the figures, it is also inferred that increase of the normalized mass, gyration radius

and attached mass position leads to decrease of the normalized frequency whereas the increase of the normalized axial load results in increase of the normalized frequency.

The normalized natural frequency of the micro-beam is depicted in figure 6 versus the ratio of the beam thickness to the material length scale parameter for three continuum theories; the classical theory, modified couple stress theory and strain gradient theory. It is noted that the two latter theories; unlike the first one; are the non-classical continuum theories capable of capturing the size-effect appearing in micro-scale structures. In addition, the two former theories are indeed special cases of the latter theory. In figure 6, the frequency evaluated by the classical, couple stress and strain gradient theory are represented by ω_{CL}, ω_{CS} and ω_{SG} respectively.

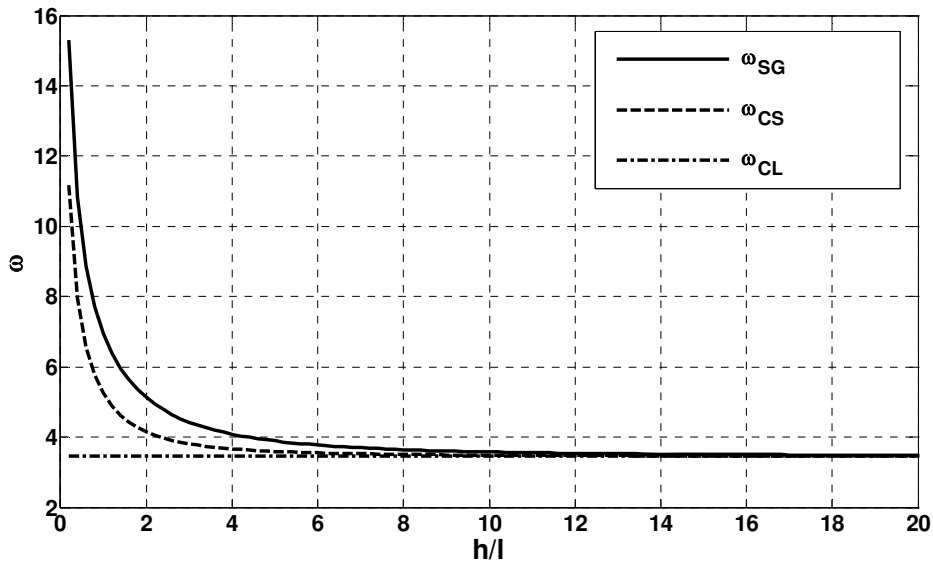


Figure 6: A comparison between the results of the strain gradient theory and those of the classical and couple stress theories.

The figure indicate that the frequency evaluated by the strain gradient theory is greater than that evaluated by the classical and couple stress theory, noted that the couple stress theory predicts higher values for the frequency than dose the classical theory. Hence, it is inferred that the micro-beams modeled by the non-classical theories are in fact stiffer than those modeled by the classical theory as it is reported by other researchers (Kong et al., 2009, Koochi et al., 2014, Vatankhah et al., 2013b). Moreover, it is deduced that the strain gradient theory predicts the micro-beams stiffer than does the couple stress theory. The figure also shows that the difference between the results of classical and non-classical theories increases as the ratio of the beam thickness to the material length scale parameter decreases. In fact, when the aforementioned ratio is greater than 10, the difference will be ignorable.

It would be helpful to evaluate the error of using the classical continuum theory instead of the non-classical theories to obtain the frequency of the micro-resonator. To that end, the relative error for the frequency is defined as:

$$error\% = \frac{\omega_{SG} - \omega_{CL}}{\omega_{SG}} \times 100\,. \tag{55}$$

The effects of the normalized axial load, mass, position of the attached mass and gyration radius together with effect of the ratio of the beam thickness to the material length scale parameter on the relative error are assessed in Figures 7-10.

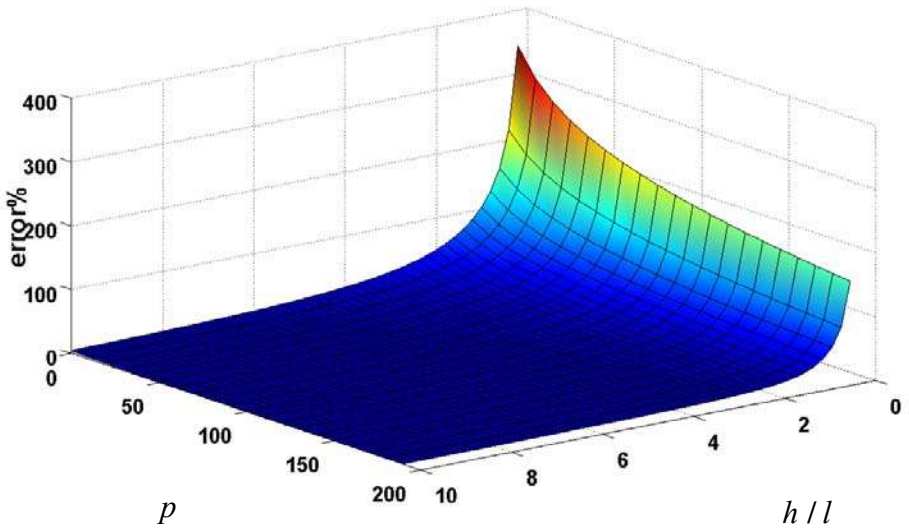


Figure 7: The relative error of the frequency as a function of the ratio of the microbeam thickness to the length scale parameter and the axial load.

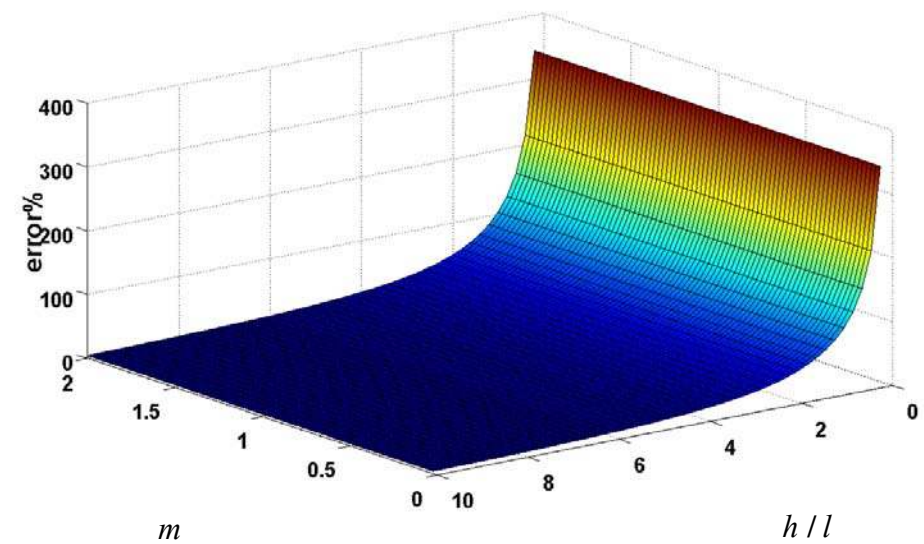


Figure 8: The relative error of the frequency as a function of the ratio of the microbeam thickness to the length scale parameter and the mass.

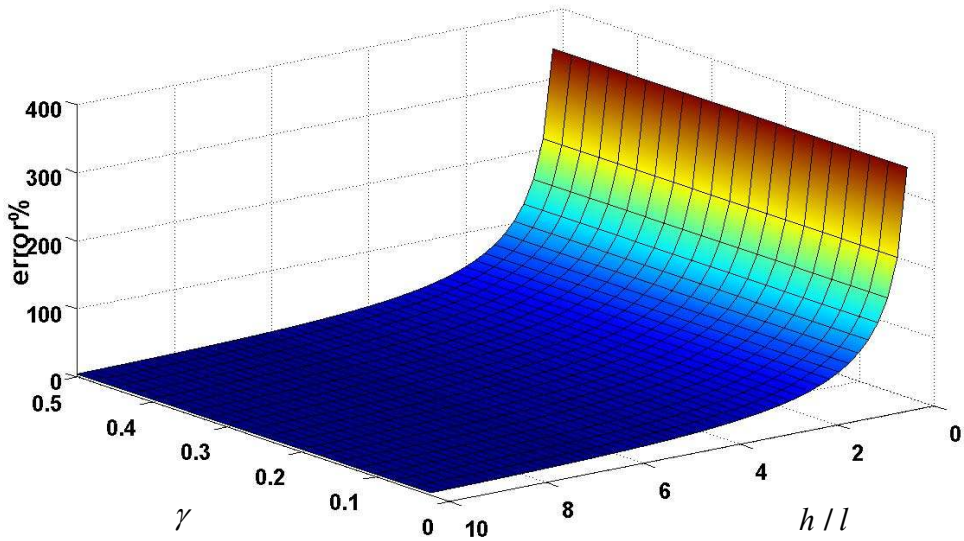


Figure 9: The relative error of the frequency as a function of the ratio of the microbeam thickness to the length scale parameter and the position of the attached mass.

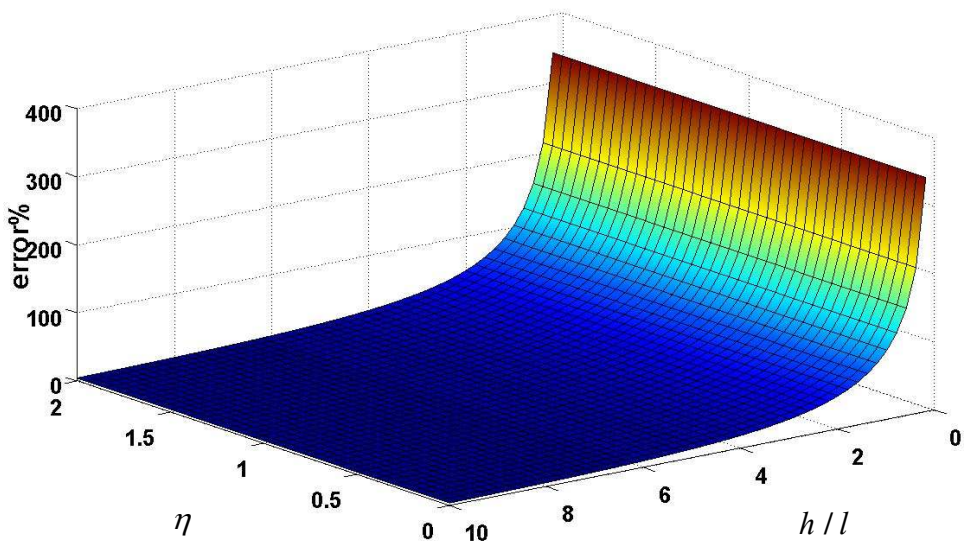


Figure 10: The relative error of the frequency as a function of the ratio of the microbeam thickness to the length scale parameter and the gyration radius of the attached mass.

These figures indicate that relative error is significant when the ratio of the beam thickness to the length scale parameter is small but it diminishes as the ratio increases. The great values of the relative error imply that using the classical continuum theory to investigate the mechanical behavior

of micro-scale structures such as micro-resonators leads to wrong results specially, when the characteristic length of the structure, i.e. thickness, diameter, etc, is comparable to the length scale parameter. However, the strain gradient theory, as a non-classical continuum theory, is successfully able to capture the size effect happening in micro-scale structures and model the micro-resonator more accurately. The figures also indicate that the effects of the normalized mass, gyration ratio and position of the attached mass are ignorable on the relative error, whereas, the effect of the normalized axial load is tangible, specially for small values of h / l. It can be seen that as the axial load increases, the relative error decreases.

5 CONCLUSIONS

Since the attempts of the classical continuum theory to capture the size-dependency happening in the micro-scale structures have been in vain, utilizing the non-classical continuum theory to investigate the mechanical behavior of such structures seems to be crucial. The strain gradient theory, as a non-classical continuum theory, is employed in this paper in order to investigate the vibration behavior of micro-resonators. The micro-resonator is modeled as a clamped-clamped beam with an attached mass subjected to an axial force. To obtain the natural frequencies of the system, it is assumed that the micro-resonator comprises two microbeams; one is located at the left-side of the attached mass while the other is at the right-side. The governing equations of motions of each beam are derived individually. Afterward, the appropriate boundary and continuity conditions are applied in order to obtain the natural frequencies of the micro-resonator. The effects of some parameters including: normalized, mass, axial load, position of the attached mass, gyration radius of the attached mass and the ratio of the beam thickness to the material length scale parameter are assessed on the normalized frequency of the micro-resonator. Furthermore, the results of the strain gradient theory are compared to those of the modified couple stress and classical continuum theories. The results can be outlined as:

- The vibration behavior of micro-resonators is size-dependent.
- The frequency of the micro-resonator increases as the ratio of the microbeam thickness to the length scale parameter decreases.
- The axial load has an increasing effect on the frequency while the effects of the mass, gyration radius and position of the attached mass are decreasing.
- The non-classical theories predict stiffer microbeams (beams with greater frequencies) than does the classical continuum theory.
- The microbeams modeled by the strain gradient theory are stiffer than those developed by the modified couple stress theory.
- The relative error of using the classical theory to model the micro-resonators is significant, especially when the microbeam thickness is comparable with its length scale parameter.
- The difference between the classical and non-classical results diminishes as the ratio of the beam thickness to the length scale parameter increases.

References

Abadi, M.M., Daneshmehr, A.R., (2014). An investigation of modified couple stress theory in buckling analysis of micro composite laminated Euler–Bernoulli and Timoshenko beams. International Journal of Engineering Science, 75, 40-53.

Ansari, R., FaghihShojaei, A., Mohammadi, V., Gholami, R., Darabi, M.A., (2014). Size-dependent vibrations of post-buckled functionally graded Mindlin rectangular microplates. Latin American Journal of Solids and Structures, 11, 2351-2378.

Asghari, M., Kahrobaiyan, M.H., Ahmadian, M.T., (2010). A nonlinear Timoshenko beam formulation based on the modified couple stress theory. International Journal of Engineering Science 48, 1749–1761.

Asghari, M., Kahrobaiyan, M.H., Rahaeifard, M., Ahmadian, M.T., (2011). Investigation of the size effects in Timoshenko beams based on the couple stress theory. Archive of Applied Mechanics, 81 (7), 863-874.

Fleck, N.A., Muller, G.M., Ashby, M.F. , Hutchinson, J.W., (1994). Strain gradient plasticity: theory and experiment. Acta Metallurgica et Materialia 42(2), 475-487.

Ghanbari, M., Hossainpour, S., Rezazadeh, G., (2015). Study of Squeeze Film Damping in a Micro-beam Resonator Based on Micro-polar Theory. Latin American Journal of Solids and Structures, 12, 77-91.

Hassanpour, P.A., Cleghorn, W.L., Esmailzadeh, E., Mills, J.K., (2007). Vibration analysis of micro-machined beam-type resonators. Journal of Sound and Vibration 308, 287–301.

Joglekar, M.M., Pawaskar, D.N., (2011). Estimation of oscillation period/switching time for electrostatically actuated microbeam type switches. International Journal of Mechanical Sciences 53, 116-125.

Kahrobaiyan, M.H., Ahmadian, M.T., Haghighi, P., Haghighi, A., (2010). Sensitivity and resonant frequency of an AFM with sidewall and top-surface probes for both flexural and torsional modes, International Journal of Mechanical Sciences 52, 1357–1365.

Kahrobaiyan, M.H., Tajalli, S.A., Movahhedy, M.R., Akbari, J., Ahmadian, M.T., (2011). Torsion of strain gradient bars. International Journal of Engineering Science, 49, 856-866.

Kong, S., Zhou, S., Nie, Z., Wang, K., (2009). Static and dynamic analysis of micro beams based on strain gradient elasticity theory. International Journal of Engineering Science 47, 487–498.

Koochi, A., Sedighi, H.M., Abadyan, M., (2014). Modeling the size dependent pull-in instability of beam-type NEMS using strain gradient theory. Latin American Journal of Solids and Structures, 11, 1806-1829.

Lam, D.C.C., Yang, F., Chong, A.C.M., Wang, J., Tong, P., (2003). Experiments and theory in strain gradient elasticity. Journal of the Mechanics and Physics of Solids 51(8), 1477–1508.

Liang, L.N., Ke, L.L., Wang, Y.S., Yang, J., Kitipornchai, S., (2015). Flexural Vibration of an Atomic Force Microscope Cantilever Based on Modified Couple Stress Theory. International Journal of Structural Stability and Dynamics, 1540025.

Ma, H.M., Gao, X.L., Reddy, J.N., (2008). A microstructure-dependent Timoshenko beam model based on a modified couple stress theory. Journal of the Mechanics and Physics of Solids 56, 3379–3391.

McElhaney, K.W., Valssak, J.J., Nix, W.D., (1998). Determination of indenter tip geometry and indentation contact area for depth sensing indentation experiments, Journal of Materials Research 13, 1300–1306

Nix, W.D., Gao, H., (1998). Indentation size effects in crystalline materials: a law for strain gradient plasticity, Journal of the Mechanics and Physics of Solids 46, 411–425.

Padoina, E., Fonseca, J.S.O., Perondi, E.A., Menuzzi, O., (2015). Optimal placement of piezoelectric macro fiber composite patches on composite plates for vibration suppression, Latin American Journal of Solids and Structures, 12.

Park, S.K., Gao, X.L., (2006). Bernoulli–Euler beam model based on a modified couple stress theory. Journal of Micromechanics and Microengineering 16(11), 2355–2359.

Stolken, J.S., Evans, A.G., (1998). Microbend test method for measuring the plasticity length scale. Acta Materialia 46(14), 5109-5115.

Tang, M., Ni, Q., Wang, L., Luo, Y., Wang, Y., (2014). Nonlinear modeling and size-dependent vibration analysis of curved microtubes conveying fluid based on modified couple stress theory. International Journal of Engineering Science, 84, 1-10.

Tsiatas, G.C., (2009). A new Kirchhoff plate model based on a modified couple stress theory. International Journal of Solids and Structures 46, 2757–2764.

Vatankhah, R., Kahrobaiyan, M.H., Alasty, A., Ahmadian, M.T., (2013b). Nonlinear forced vibration of strain gradient microbeams. Applied Mathematical Modelling, 37, 8363-8382.

Vatankhah, R., Najafi, A., Salarieh, H., Alasty, A., (2013a). Boundary stabilization of non-classical micro-scale beams. Applied Mathematical Modelling, 37, 8709-8724.

Vatankhah, R., Najafi, A., Salarieh, H., Alasty, A., (2014a). Exact boundary controllability of vibrating non-classical Euler–Bernoulli microscale beams. Journal of Mathematical Analysis and Applications, 418, 985-997.

Vatankhah, R., Najafi, A., Salarieh, H., & Alasty, A. (2014b). Asymptotic decay rate of non-classical strain gradient Timoshenko micro-cantilevers by boundary feedback. Journal of Mechanical Science and Technology, 28(2), 627-635.

Vatankhah, R., Karami, F., & Salarieh, H. (2015a). Observer-based vibration control of non-classical microcantilevers using extended Kalman filters. Applied Mathematical Modelling, 39, 5986–5996.

Vatankhah, R., Najafi, A., Salarieh, H., & Alasty, A. (2015b). Lyapunov-Based Boundary Control of Strain Gradient Microscale Beams With Exponential Decay Rate. Journal of Vibration and Acoustics, 137(3), 031003.

Wang, K.F., Kitamura, T., Wang, B., (2015). Nonlinear pull-in instability and free vibration of micro/nanoscale plates with surface energy- a modified couple stress theory model. International Journal of Mechanical Sciences, doi:10.1016/j.ijmecsci.2015.05.006.

Yang, F., Chong, A.C.M., Lam, D.C.C., Tong, P., (2002). Couple stress based strain gradient theory for elasticity. International Journal of Solids and Structures 39 (10), 2731–2743.